COMPDYN 2011
III ECCOMAS Thematic Conference on
Computational Methods in Structural Dynamics and Earthquake Engineering
M. Papadrakakis, M. Fragiadakis, V. Plevris (eds.)
Corfu, Greece, 25–28 May 2011

INVESTIGATION OF COUPLING BETWEEN EXTERNAL AND PARAMETRIC RESONANCES IN SMALL SAGGED INCLINED CABLES

Cyril E. Douthe[1,2], Charis J. Gantes[1]

[1] National Technical University of Athens
Metal Structures Laboratory, 9 Heroon Polytechniou, 15780 Zographou, Greece
e-mail: chgantes@central.ntua.gr

[2] Université Paris-Est
IFSTTAR, Dép. Structures et Ouvrages d'Art (Pt 34), 58, Bd Lefebvre, 75732 Paris Cedex 15, France
e-mail: cyril.douthe@ifsttar.fr

Keywords: Stay cable, modal interaction, method of harmonic balance, instability zone, threshold amplitude.

Abstract: *The coupling between parametric and external resonances in inclined cables subjected to a motion of an anchorage with components both along and perpendicular to their axis is investigated. Besides posing theoretical challenges, this problem is of practical interest for inclined cables of cable-stayed bridges and guyed towers. First, the state of the art on the subject of multi-modal interactions of cables with moving anchorages is summarized. Then, the proposed analytical model is presented, which is selected to be as simple as possible, but still suitable for capturing the coupling between the first and second eigenmodes, hence between parametric and external resonances. Next, two specific cases of the general model, in which no coupling appears, are studied in order to identify the intrinsic characteristics of external and parametric resonance, respectively. Finally, the coupling between the two instabilities is investigated, aiming at a better understanding of the interaction phenomenon and at formulating practical engineering guidelines.*

1 STATE-OF-ART ON MULTI-MODAL VIBRATIONS OF CABLES

In cable stayed bridges or guyed towers, indirect excitation through the vibrations of the neighboring structural elements, the bridge deck and the tower respectively, can lead to oscillations with high amplitudes in case resonance takes place. This resonance may be external, parametric or a combination of both. External resonance is induced by a motion of the anchorage perpendicular to the cable axis and occurs when the exciting frequency is equal to any eigenfrequency of the cable. Parametric resonance describes the dynamic instability which is induced by a motion of the anchorage along the axis of the cable and is observed when the ratio between the exciting frequency and some eigenfrequency takes specific values like 2:1, 3:1, 1:2 or 1:3.

The phenomenon of external resonance is well known among bridge designers and many design guidelines of cable stayed bridges provide a description of it and propose measures to prevent its effects [1, 2]. Most current models are linear [1, 2], but models including cubic non-linearities exist, like Irvine's solution for undamped motion (chapter 3.4 of [3]) or that of Caetano including damping [4]. The phenomenon of parametric resonance has entered the structural engineers' culture more recently with the development of the new generation of cable stayed bridges [5], it is hence detailed in [2] but only mentioned in [1]. It has been described first by Kovacs [6]. Then, Uhrig [7] proposed the first expressions of the main instability zones for the excitation frequencies in which the response diverges. Lilien and Pinto da Costa [8], in parallel with Cai and Chen [9], established the first values of the amplitude of the non-linear response in the main instability zone, the so-called two to one (2:1) resonance. These results were confirmed by Clément and Crémona using the harmonic balance method [10] and by Berlioz and Lamarque using the multiple scales method [11]. Takahashi [12] has shown that there were many instability zones around the multiples of the cable eigenfrequencies but also in the neighborhood of combinations of those, the so-called combination resonances.

The interaction between external and parametric resonance has been studied using different approximations depending on the sag of the cable, as outlined in Rega's bibliographical report [13]. A detailed literature review for coupled external-parametric resonances for taut strings can be found in Nayfeh and Mook [14]. The first studies of modal interaction in sagged cables concern internal resonances [15] or the coupled response to distributed load [16, 17, 18]. Luongo *et al.* have shown that, when the sag is significant, quadratic non-linearities govern the response while cubic non-linearities dominate when the sag is small [15, 19]. For instance, the publications on uncoupled parametric resonance cited above [6, 12, 7, 8, 9, 10, 11] concern only small sagged cables and include only cubic non-linearities.

A two degrees of freedom model for in-plane external resonance / out-of-plane parametric resonance interaction of large sagged cables was proposed by Perkins [20]. He observed that, like for taut strings, for small exciting amplitudes the system is uncoupled but, when the amplitude exceeds a certain value, parametric resonance occurs and the system becomes coupled. Gonzalez-Buelga *et al.* extended this model by taking into account the second out-of-plane mode in the response, but they limited themselves to small sagged cables [21]. Two mode planar interaction was also studied by Chatjigeorgiou and Mavrakos in a marine context [22], including small bending stiffness and quadratic damping due to fluid drag forces. A four degrees of freedom model for a large sagged cable was studied by Benedettini and Rega [23]. Zhang and Tang investigated also multi-modal interaction, focusing on the bifurcation type and on the response to chaotic excitation [24]. Multi-modal interaction was also studied by Srinil and Rega who compared finite differences numerical results with multiple scales analytical results (with up to 15 modes), in order to check if simulations can capture the richness of the cable's behavior near the first cross-over region undergoing 1:1 or 2:1

resonance [25]. Srinil and Rega also investigated the accuracy of reduced order models for the modeling of 2:1 resonance in horizontal and inclined cables. They showed that "the minimal (two-degrees-of-freedom) model" involving only the resonant modes seems capable of providing reliable results only for very low-sagged cables [26].

Advanced multi-modal models are thus nowadays available for researchers studying the dynamic interaction of sagged cables excited parametrically. These models try to take into account the whole complexity of the problem (generally in a relatively theoretical manner), the problem of coupled external/parametric resonance of small sagged cables being treated as a simple specific case. There is, however, need for a coupled model of small sagged cables for structural design of stay cables in engineering practice, in order to identify clearly the instability regions and the amplitude of responses. Gonzalez-Buelga *et al.* made a first step in this direction using the multiple scales method for out-of-plane parametric resonance [21]. For small sag however, the frequencies of in-plane and out-of-plane symmetric modes are very close, so that there might be internal resonance. It is thus proposed here to study the relative influence of in-plane and out-of-plane parametric resonance and its coupling with in-plane external resonance. In section 2 an analytical model is developed based on the harmonic balance method and compared with finite element numerical results. Uncoupled external and parametric resonances are studied in the third and fourth section, respectively, in order to identify their characteristics. The fifth section is dedicated to the study of the coupled problem.

2 DEVELOPMENT OF THE ANALYTICAL MODEL

2.1 Presentation of the problem

The analytical model presented here is dedicated to the study of multi-modal non-linear vibrations of inclined cables subjected to coupled external/parametric resonance. One end of the cable is fixed while the other end is subjected to an imposed motion (figure 1). This situation could correspond to a cable of a cable stayed bridge with the upper end fixed on a stiff pylon and the lower end supporting a flexible deck. The imposed motion of the lower end could be due to wind or traffic induced vibration of the deck. The cable is assumed to have small sag, which is a realistic assumption for bridge cables.

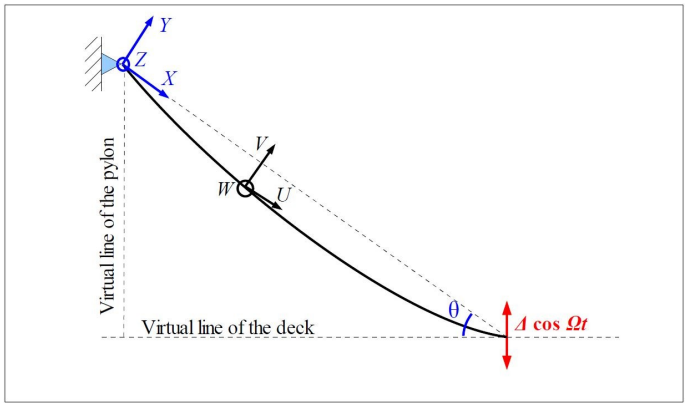

Figure 1: Inclined cable submitted to harmonic excitation at one end.

The plane of the cable is described by coordinates X, along the line joining the two ends of the cable and Y, perpendicular to this line, with the origin located at the fixed end. The out-of-plane coordinates are represented by Z. The inclination of the cable axis with respect to the virtual line of the deck (which is here supposed to be horizontal) is denoted by the angle θ. Without loss of generality, the imposed motion is supposed to be vertical and harmonic with

amplitude Δ and frequency Ω, called respectively exciting amplitude and exciting frequency. All other forces except gravity are neglected. As noted above, it is further assumed that the sag of the cable is small, so that the difference between the abscissa along the cable and the abscissa along the chord can be neglected. Another consequence of the small sag is that the static equilibrium shape of the cable, which is in reality a catenary, can be assumed as parabolic [5].

2.2 Derivation of equations of motion

For common stay cables, axial displacements are much smaller than transverse displacements, so that here only displacements in the Y and Z directions will be considered and denoted as $V(X,t)$ and $W(X,t)$, respectively. The equations of motion being non-linear, their solutions are generally derived using Galerkin's method [20, 23, 10, 24, 11, 21]. Considering previous investigations by Gonzalvez Buena *et al.* [21] and the targeted field of application (small sagged stay cables), the present study is limited to the first out-of-plane mode, the first in-plane mode and the second in-plane mode. The approximate displacements are thus expressed as:

$$v(x,t)=p_1(t)\sin(\pi x)+p_2(t)\sin(2\pi x)+\delta\cos(\Omega t)x\cos\theta \tag{1a}$$

$$w(x,t)=q_1(t)\sin(\pi x) \tag{1b}$$

where p_1 and p_2 are time functions corresponding to the first and second in-plane mode, and q_1 that of the first out-of-plane mode. Note that in the previous expressions, the various parameters have been expressed in a dimensionless form with respect to the length of the cable:

$$x=\frac{X}{L}\ ,\ \delta=\frac{\Delta}{L}\ ,\ v=\frac{V(X,t)}{L}\ \text{and}\ w=\frac{W(X,t)}{L} \tag{2}$$

Considering the small sag of the cable, the eigenfrequencies are obtained following the approximation proposed by Gonzalvez Buena *et al.* [21] and are given by:

$$\omega_i^{\text{in}} = \frac{\pi i}{L}\sqrt{\frac{T}{\rho}}\sqrt{1+\frac{2\lambda^2}{i^4\pi^4}\left[1+(-1)^{i+1}\right]^2}\ ,\ \omega_j^{\text{out}} = \frac{\pi j}{L}\sqrt{\frac{T}{\rho}} \tag{3}$$

where T is the tension in the cable (which is assumed constant along the length), ρ its mass per unit length and λ the so-called Irvine's parameter, which is generally smaller than 1, except for very large cable stayed bridges; it is given in terms of the elastic modulus E of the cable, its cross-sectional area S and the gravity acceleration g:

$$\lambda^2 = \frac{E\,S}{T}\cdot\left(\frac{\rho\,L\,g\cos\theta}{T}\right)^2 \tag{4}$$

Following then the procedure proposed by Luongo *et al.* [15], the quadratic terms in the equations of motion are neglected. Looking at the remaining equations, one observes that the roles played by the first in-plane mode p_1 and by the first out-of-plane mode q_1 are identical. Moreover, previous experiments on taut cables have shown that only one of the two modes has a nonzero amplitude [11, 20, 21] (in general only the out-of-plane mode occurs). So, for simplicity reasons, only one of the two modes will be considered. The equations of motion reduce hence to:

$$\ddot{p}_1+2\,\xi\,\omega_1\dot{p}_1+\omega_1^2(1+2\,a\cos\Omega t)\,p_1+c_3\,p_1(p_1^2+4\,p_2^2) = 0 \tag{5a}$$

$$\ddot{p}_2+\xi\,\omega_2\dot{p}_2+\omega_2^2(1+2\,a\cos\Omega t)\,p_2+4\,c_3\,p_2(p_1^2+4\,p_2^2) = F_2(t) \tag{5b}$$

where ω_1 denotes, indifferently, the frequency of the first out-of-plane mode ω_1^{out} or that of the first in-plane mode ω_1^{in}. ξ is the modal damping ratio of the first out-of-plane mode which is assumed identical to that of the first in-plane mode and equal to twice that of the second mode. The dimensionless amplitude a of parametric excitation, the coefficient of the cubic terms c_3 and that of external excitation in-plane F_2 are given respectively by:

$$a = \frac{ES}{2T}\delta \sin\theta \ , c_3 = \frac{\pi^2}{4}\frac{ES}{T}\omega_1^2 \text{ and } F_2(t) = -\frac{\delta \cos\theta \Omega^2}{\pi}\cos(\Omega t) \tag{6}$$

2.3 Method of harmonic balance

In equations (5a) and (5b), the coupling is limited to the non-linear terms. For this reason, the coupling will have an influence only near resonance conditions. Previous research [20, 23, 27] has indeed shown that the instability regions were only marginally affected by the coupling. Thus, the exciting frequencies, which might cause instability of the cable, are:

- $\Omega \approx 2\ \omega_1$ for the first in-plane or out-of-plane mode (parametric resonance);
- $\Omega \approx \omega_2$ for the second in-plane mode (external resonance).

As, for small sagged cables, these three frequencies are close to each other, interactions between parametric resonance in-plane or out-of-plane and external resonance in-plane might appear. The present study will thus be limited to a frequency region in the vicinity of the frequency of the second in-plane mode. In this region, it can be assumed that the time functions p_1 and p_2 are of the following form [10]:

$$p_1(t) = p_{11}\sin(\Omega t/2) + p_{12}\cos(\Omega t/2) \tag{7a}$$

$$p_2(t) = p_{21}\sin(\Omega t) + p_{22}\cos(\Omega t) \tag{7b}$$

where p_{11}, p_{12}, p_{21}, and p_{22} are real numbers, which will be determined later.

Introducing these terms into (5a) and (5b) and using the method of harmonic balance (which allows us to neglect the terms of high frequencies), leads finally to a system of four equations with four unknowns (p_{11}, p_{12}, p_{21} and p_{22}). This system can be separated into two matrix equations, which are characteristic of the coupled problem of inclined cables submitted to a harmonic motion at one end:

$$\begin{bmatrix} \frac{3}{4}c_3A^2 + 2c_3B^2 + \omega_1^2 a + \omega_1^2 - \frac{\Omega^2}{4} & -\xi\omega_1\Omega \\ \xi\omega_1\Omega & \frac{3}{4}c_3A^2 + 2c_3B^2 - \omega_1^2 a + \omega_1^2 - \frac{\Omega^2}{4} \end{bmatrix} \cdot \begin{bmatrix} p_{11} \\ p_{12} \end{bmatrix} = \begin{bmatrix} 0 \\ 0 \end{bmatrix} \tag{8a}$$

$$\begin{bmatrix} 2c_3A^2 + 12c_3B^2 + \omega_2^2 - \Omega^2 & -\xi\omega_2\Omega \\ \xi\omega_2\Omega & 2c_3A^2 + 12c_3B^2 + \omega_2^2 - \Omega^2 \end{bmatrix} \cdot \begin{bmatrix} p_{21} \\ p_{22} \end{bmatrix} = \begin{bmatrix} 0 \\ -\delta\cos\theta\Omega^2/\pi \end{bmatrix} \tag{8b}$$

where $A^2 = p_{11}^2 + p_{12}^2$ and $B^2 = p_{21}^2 + p_{22}^2$.

3 UNCOUPLED EXTERNAL RESONANCE

3.1 Characteristic equation of uncoupled external resonance

Before studying the coupled system, the problems of external resonance and parametric resonance are treated separately, in order to understand better their characteristics. The study of external resonance is generally concerned with the response to an excitation according to the first mode of vibration, while here focus will be on the second in-plane mode of vibration,

which is susceptible to interact with parametric resonance terms when coupling is considered. Thus, considering a horizontal cable subjected to a vertical excitation at one end, the amplitude of the first mode vanishes in expression (8b) ($A = 0$) and one obtains the following system of equations, which is characteristic of the uncoupled external resonance:

$$\begin{bmatrix} 12c_3B^2+\omega_2^2-\Omega^2 & -\xi\omega_2\Omega \\ \xi\omega_2\Omega & 12c_3B^2+\omega_2^2-\Omega^2 \end{bmatrix} \cdot \begin{bmatrix} p_{21} \\ p_{22} \end{bmatrix} = \begin{bmatrix} 0 \\ -\delta\cos\theta\,\Omega^2/\pi \end{bmatrix} \tag{9}$$

To solve the above equation, it is necessary to check under what conditions the determinant of the matrix is different from zero:

$$144c_3^2B^4+24c_3(\omega_2^2-\Omega^2)B^2+(\omega_2^2-\Omega^2)^2+\xi^2\omega_2^2\Omega^2 = 0 \tag{10}$$

This is a bi-quadratic equation which has real solutions if and only if its discriminant is positive. As it is always negative, the matrix in (9) can be inverted and a third degree polynomial equation linking the square amplitude of the response B^2 with the amplitude of the excitation δ is obtained:

$$144c_3^2B^6+24c_3(\omega_2^2-\Omega^2)B^4+\left[(\omega_2^2-\Omega^2)^2+\xi^2\omega_2^2\Omega^2\right]B^2-\delta^2\cos^2\theta\frac{\Omega^4}{\pi^2} = 0 \tag{11}$$

The real roots of (11) can be calculated with the method of Cardan. Depending on the value of the parameters, equation (11) might have one or three real roots, out of which only two are stable amplitudes of response.

3.2 Characteristics of the hysteresis region

The interval of exciting amplitudes for which two stable amplitudes exist is called hysteresis region, because of the role played by the state of the cable at the preceding time in the determination of the actual amplitude. The limits of the hysteresis region can be determined from the characteristic equation of external resonance (11), which can be rewritten in a more concise manner:

$$k_1Y^3+k_2Y^2+k_3Y+k_4=0 \tag{12}$$

where:

$$k_1 = 144c_3^2,\ k_2 = 24c_3(\omega_2^2-\Omega^2),\ k_3 = (\omega_2^2-\Omega^2)^2+\xi^2\omega_2^2\Omega^2 \text{ and } k_4 = -\delta^2\cos^2\theta\,\Omega^4/\pi^2 \tag{13}$$

Equation (12) has three real solutions if and only if its discriminant is positive. The borders of the hysteresis region are thus given by the parameters which nullify this discriminant. After some standard algebraic manipulations, one finally finds the expressions of the two critical exciting amplitudes, which limit the hysteresis region:

$$\delta_1 = \frac{\pi}{\cos\theta\,\Omega^2}\sqrt{\frac{1}{27}k_2\left[2\left(\frac{k_2}{k_1}\right)^2-9\frac{k_3}{k_1}\right]-\frac{k_1}{\sqrt{2}}\left[\frac{2}{9}\left(\frac{k_2}{k_1}\right)^2-\frac{2k_3}{3k_1}\right]^{\frac{3}{2}}} \tag{14a}$$

$$\delta_2 = \frac{\pi}{\cos\theta\,\Omega^2}\sqrt{\frac{1}{27}k_2\left[2\left(\frac{k_2}{k_1}\right)^2-9\frac{k_3}{k_1}\right]+\frac{k_1}{\sqrt{2}}\left[\frac{2}{9}\left(\frac{k_2}{k_1}\right)^2-\frac{2k_3}{3k_1}\right]^{\frac{3}{2}}} \tag{14b}$$

The critical frequency Ω_{cr} for which more than one solutions exist, is given by the intersection of the two curves resulting from (14a) and (14b). This frequency, which is higher than the frequency of the second eigenmode ($\Omega_{cr} > \omega_2$), can be evaluated using (13), (14a) and (14b):

$$\Omega_{cr} = \omega_2 \sqrt{1+\frac{3}{2}\xi^2+\frac{\xi}{2}\sqrt{12+9\xi^2}} \tag{15}$$

Expressions (14a), (14b) and (15) allow us to define four regions, each corresponding to a different nature of the response to external resonance. These regions are represented in figure 2 for excitation parameters in dimensionless forms:

- $\Omega < \Omega_{cr}$: The response is undifferentiated, the highest the frequency and the amplitude of excitation, the higher the amplitude of the response;
- $\Omega > \Omega_{cr}$ and $\delta < \delta_1$: Low external resonance occurs, small amplitude response;
- $\Omega > \Omega_{cr}$ and $\delta > \delta_2$: High external resonance occurs, large amplitude response;
- $\Omega > \Omega_{cr}$ and $\delta_1 < \delta < \delta_2$: Hysteresis region, high external resonance might occur, depending on the time history of the excitation; two amplitudes, one small and one large, are thus possible.

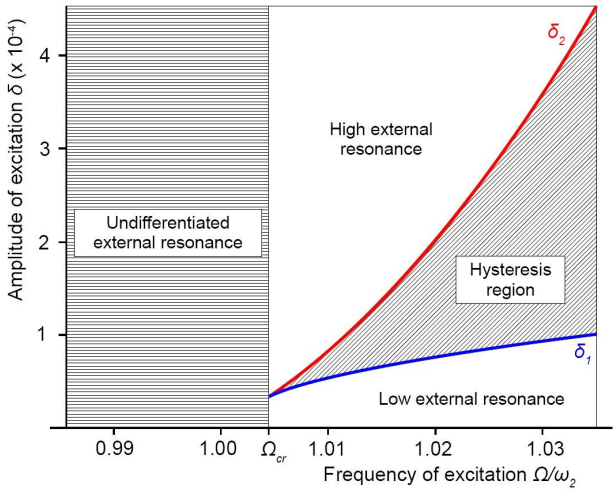

Figure 2: Nature of the response to external resonance.

3.3 Practical example: a cable of the Ben-Ahin Bridge

To illustrate the expressions found in the previous sub-section, some results are shown based on the geometric and mechanical properties of a cable of the Ben-Ahin Bridge in Belgium, which was abundantly studied by Da Caetano [5]. Its main characteristics are all supposed constant along its length and are the following:

- Length: L = 110.505 m (distance between the anchorages);
- Mass per unit length: ρ = 64.841 kg/m;
- Cross-sectional area: S = 82.6 cm^2;
- Young Modulus: E = 210 GPa ;
- Prestress: T = 4902.7 kN (actually the prestress is not exactly constant in the numerical model due to gravity; the value given here is that at the lower anchorage).

From those values, the parameters characterizing the vibrations of the horizontal cable can be evaluated: Irvine's parameter λ^2 = 0.0727, the frequency of the 1st out-of-plane mode ω_1^{out} = 7.82 rad/s, the frequency of the first in-plane mode ω_1^{in} = 7.84 rad/s. One remarks that the value of Irvine's parameter of this cable is very low, therefore, the cable is small sagged.

The finite element software used to validate the analytical model and its hypotheses is ADINA, a software which has already been successfully used for the calculation of cable structures [27, 28]. A convergence study in time and space was first conducted for a horizontal cable subjected to gravity and to an excitation perpendicular to its axis with a

frequency equal to that of the second in-plane eigenmode and an amplitude of 10 mm. Rayleigh damping proportional to the mass is chosen, because this is what is generally used for the modeling of cables and because it is the numerical damping which is the closest to the analytical model (in the present example $\xi = 0.5$ %). Geometrical non-linearities are taken into account and the default implicit dynamic algorithm based on Newmark integration method is used with a consistent mass matrix. The time step is varied from 1 ms to 10 ms and the number of elements from 30 to 100. The calculations are separated into two parts: the transient period, from 0 s to 300 s, and the steady state, from 300 s and 340 s. From the variations of the amplitude of the steady state response, 40 truss elements and $\Delta t = 5$ ms was chosen as the best compromise between computation time and accuracy.

Then the results of the numerical model were compared with those of the analytical model for an excitation of $\Delta = 20$ mm. They globally showed very good agreement and the differences in the steady state amplitude varied from 1.5 % for $\Omega = \omega_2$ to 5 % for $\Omega = 1.05\ \omega_2$.

4. UNCOUPLED PARAMETRIC RESONANCE

The phenomenon of parametric resonance is relatively well known from the literature but it is often not distinguished between in-plane and out-of-plane resonance. As, for small sagged cables, the frequency of the first out-of-plane mode is very close to that of the first in-plane mode (a few percentage points in cables of cable stayed bridges), they might often be confused. Therefore, it is meaningful to study the phenomenon and to look for a possible internal resonance between the first in-plane and out-of-plane modes.

4.1 Analytical expression of the amplitude and the threshold

The equations of uncoupled parametric resonance are often found by taking into account only the first in-plane mode in the general equations of motion [8], [10]. Here, the first in-plane and first out-of-plane modes will be considered alternatively (ω_1 representing either the frequency of the first in-plane or first out-of-plane mode) and the characteristic equation of parametric resonance is deduced from (8a) by considering that the cable is horizontal and submitted to a horizontal motion ($B = 0$):

$$\begin{bmatrix} \frac{3}{4}c_3A^2-\omega_1^2a+\omega_1^2-\frac{\Omega^2}{4} & -\xi\omega_1\Omega \\ \xi\omega_1\Omega & \frac{3}{4}c_3A^2+\omega_1^2a+\omega_1^2-\frac{\Omega^2}{4} \end{bmatrix} . \begin{bmatrix} p_{11} \\ p_{12} \end{bmatrix} = \begin{bmatrix} 0 \\ 0 \end{bmatrix} \tag{16}$$

This problem has a nonzero solution, if the determinant of the matrix is equal to zero:

$$\frac{9}{16}c_3^2A^4+\frac{3}{2}c_3(\omega_1^2-\frac{\Omega^2}{4})A^2+\xi^2\omega_1^2\Omega^2-\omega_1^4a^2+\left(\omega_1^2-\frac{\Omega^2}{4}\right)^2 = 0 \tag{17}$$

One recognizes in (17) a bi-quadratic equation in A. It has real solutions if and only if its discriminant is larger than or equal to zero, which is equivalent to the following condition:

$$a^2\omega_1^2-\xi^2\Omega^2 \geqslant 0 \tag{18}$$

Equation (18) determines a first condition on the instability zone: for a given exciting frequency Ω, as long as the dimensionless amplitude of the excitation is below a certain threshold $a^2 < \xi^2\Omega^2/\omega_1^2$, there is no instability and the only solution of the problem of parametric excitation is zero ($p_{11} = p_{12} = 0$); on the contrary, when the exciting amplitude reaches the limit amplitude $a^2 \geqslant \xi^2\Omega^2/\omega_1^2$, equation (17) has two solutions and the characteristic amplitudes of uncoupled parametric resonance A_U are given by:

$$A_U = \sqrt{\frac{4}{3}\frac{\omega_1^2}{c_3}} \cdot \sqrt{\left(\frac{\Omega}{2\omega_1}\right)^2 - 1 \pm \sqrt{a^2 - 4\xi^2\left(\frac{\Omega}{2\omega_1}\right)^2}} \tag{19}$$

One remarks that the limit case $a^2 = \xi^2\Omega^2/\omega_1^2$ corresponds to the pair "exciting amplitude/ exciting frequency" for which the two characteristic amplitudes of uncoupled parametric resonance (19) are equal. For a given exciting amplitude, this frequency is the highest frequency for which parametric resonance may occur. It is also the frequency for which the amplitude of parametric resonance is the highest. It is noted also that condition (18) is not sufficient for appearance of parametric resonance: the expression under the square root in (19) has to be positive. It is, thus, necessary for the dimensionless amplitude of parametric excitation to be higher than a certain critical value a_U which is often called the threshold of parametric excitation:

$$a_U = \sqrt{\left[\left(\frac{\Omega}{2\omega_1}\right)^2 - 1\right]^2 + 4\xi^2\left(\frac{\Omega}{2\omega_1}\right)^2} \tag{20}$$

Another way to look at this condition, on the dimensionless amplitude of excitation, is to rewrite (20) as a condition on the exciting frequency:

$$\Omega \in \left[2\omega_1\sqrt{1 - 2\xi^2 - \sqrt{a^2 - 4\xi^2(1-\xi^2)}} \;,\; 2\omega_1\sqrt{1 - 2\xi^2 + \sqrt{a^2 - 4\xi^2(1-\xi^2)}}\right] \tag{21}$$

4.2 Numerical study of amplitudes and thresholds

As the influences of damping ratio, frequency and exciting amplitude have been studied abundantly in the past (for example in [10]), it is here focused on the interaction between in-plane and out-of-plane parametric resonance. A first model, in which a horizontal cable identical to the one in section 3.3 has an anchorage moving horizontally, is hence considered. It is then modified for the out-of-plane instability by introducing at time zero an out-of-plane perturbation in the form of a small vanishing wind gust, uniformly distributed along the cable. The variations of the amplitude of both responses with the frequency of the excitation are shown in figure 3a for $\Delta = 20$ mm and $\xi = 0.08$ %. The amplitudes of the response plotted in this figure are steady state amplitudes obtained after a transient period of 1000 cycles. It is observed that there is very good agreement between numerical and analytical results for both in-plane and out-of-plane response for the stable branches (corresponding to growing frequencies). There is also good agreement of the frequency of the jump phenomenon (obtained with a decreasing frequency) for the in-plane numerical simulations; but, numerically, the frequency of the out-of-plane jump coincides with the frequency of the in-plane jump.

From this last observation, one may suppose that the in-plane vibration is not stable and turns into out-of-plane vibration when it is disturbed. Indeed, every time that a small out-of-plane perturbation is introduced in a plane model where in-plane parametric resonance is installed, out-of-plane resonance appears and then gradually dominates the whole response and the in-plane vibration vanishes.

These results are confirmed when investigating more specifically the threshold amplitudes of the out-of-plane mode (figure 3b). Two damping factors are tested ($\xi = 0.1$ % and $\xi = 0.5$ %) and both sets of simulations lead to similar results. Figure 3b represents the threshold amplitudes for $\xi = 0.5$ %. For low frequencies, there is very good agreement between analytical and numerical results for both the in-plane and the out-of-plane threshold. For high frequencies, numerical results for the in-plane and out-of-plane threshold coincide and are in very good agreement with the analytical values of the in-plane mode. The in-plane

mode of vibration is unstable and turns into out-of-plane vibration. These results should be confirmed for other values of Irvine's parameter, thus, with other ratios between in-plane and out-of-plane frequencies. Yet, it seems that the amplitude of the response which should be taken into account is that of the out-of-plane mode and that the following bandwidth of parametric resonance has to be considered:

$$\Omega \in I^{\text{in}} \cup I^{\text{out}} \quad \text{where} \quad \begin{aligned} I^{\text{in}} &= \left[2\omega_1^{\text{in}}\sqrt{1-2\xi^2-\sqrt{a^2-4\xi^2}}, 2\omega_1^{\text{in}}\sqrt{1-2\xi^2+\sqrt{a^2-4\xi^2}}\right] \\ I^{\text{out}} &= \left[2\omega_1^{\text{out}}\sqrt{1-2\xi^2-\sqrt{a^2-4\xi^2}}, 2\omega_1^{\text{out}}\sqrt{1-2\xi^2+\sqrt{a^2-4\xi^2}}\right] \end{aligned} \tag{22}$$

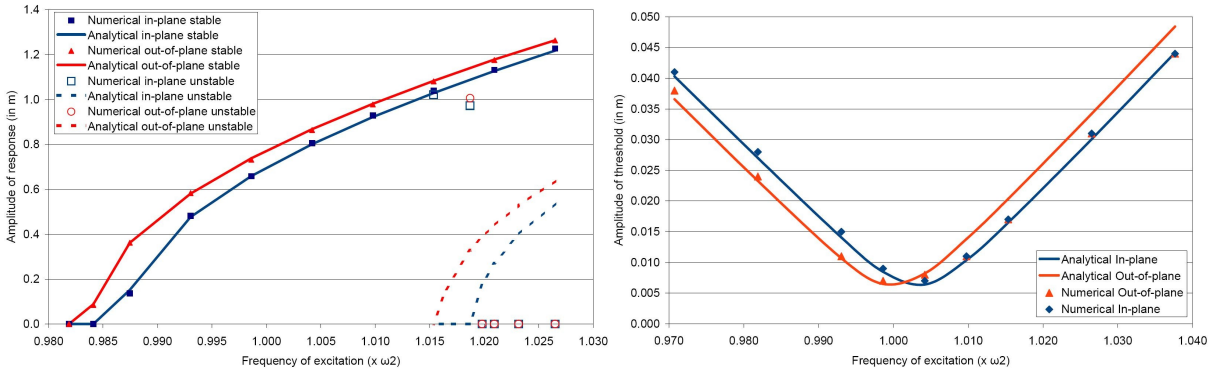

Figure 3: Influence of the excitation frequency
a) on the amplitude of in-plane and out-of-plane parametric resonance, b) on the corresponding thresholds.

5. COUPLED EXTERNAL/PARAMETRIC RESONANCE

5.1 Coupled threshold of parametric resonance

5.1.1 Analytical expression

Considering now the coupled system of equations (8a) and (8b), equation (8a) will be studied first. This system of equations is homogeneous, so that it has nonzero solutions if and only if the determinant of the matrix is equal to zero, which is equivalent to requiring that solutions of the following equation can be found:

$$\frac{9}{16}c_3^2A^4+3\frac{c_3}{2}\left[2c_3B^2+\left(\omega_1^2-\frac{\Omega^2}{4}\right)\right]A^2+\left[\omega_1^2-\frac{\Omega^2}{4}+2c_3B^2\right]^2-\omega_1^4a^2+\xi^2\omega_1^2\Omega^2 = 0 \tag{23}$$

A bi-quadratic equation in A can be recognized in (23) and thus, the first condition for the existence of real roots to this equation is that its discriminant is equal to zero:

$$a^2\omega_1^2-\xi^2\Omega^2 > 0 \tag{24}$$

It is noteworthy that this condition is identical to the one obtained for the uncoupled problem (18): the highest frequency for which parametric resonance may appear is thus identical for the coupled and the uncoupled problem. As previously, if the non-dimensional amplitude of parametric excitation is higher than a certain threshold ($a > \xi\,\Omega/\omega_1$), then the solution of (23) can be written:

$$A=\sqrt{-\frac{8}{3}B^2+\frac{4}{3}\frac{\omega_1^2}{c_3}\left[\left(\frac{\Omega}{2\omega_1}\right)^2-1\pm\sqrt{a^2-4\xi^2\left(\frac{\Omega}{2\omega_1}\right)^2}\right]} \quad \left(=\sqrt{A_U^2-\frac{8}{3}B^2}\right) \tag{25}$$

Considering (25), one remarks that like for uncoupled parametric resonance, the problem

of coupled parametric resonance has two solutions: one stable (with the positive sign under the square root) and one unstable. Like for uncoupled parametric resonance, the non-dimensional amplitude of parametric excitation has to be higher than a certain value, called threshold of coupled parametric resonance a_C. Below the threshold, no parametric resonance appears: the system is uncoupled and external resonance only may occur. Above this threshold, coupled external-parametric resonance may occur and the amplitude of the coupled parametric resonance is always smaller than that of uncoupled parametric resonance (the amplitude of the second mode reduces the amplitude of the first mode).

The value of the threshold amplitude depends thus on the history of the vibration of the cable. If the vibration starts from a non-coupled state where only external resonance exists, then when the threshold of coupled parametric resonance is just reached, the amplitude of external resonance is still the uncoupled one ($B_C = B_U$ given by (11)). On the contrary, if the vibration starts from a coupled state where both resonances exist, then, when the threshold is reached, the amplitude of external resonance is still the coupled one.

In the first case, the coupled threshold amplitude δ_{CU} can be found without solving the coupled system of equations. Its value is obtained by solving the following non-linear equation resulting from (26) with $A = 0$ and $B = B_U$ which is a stable solution of (11):

$$\delta_{CU} = \frac{2T}{ES\sin\theta}\sqrt{\left[\left(\left(\frac{\Omega}{2\omega_1}\right)^2-1\right)-\frac{2c_3}{\omega_1^2}B_U^2(\delta_{CU})\right]^2+4\xi^2\left(\frac{\Omega}{2\omega_1}\right)^2} \tag{26a}$$

In the second case, it is necessary to solve the coupled system of equations and to obtain the value of the coupled amplitude B_C in order to introduce it in the expression of the threshold amplitude which is then given by:

$$\delta_{CC} = \frac{2T}{ES\sin\theta}\sqrt{\left[\left(\left(\frac{\Omega}{2\omega_1}\right)^2-1\right)-\frac{2c_3}{\omega_1^2}B_C^2(\delta_{CC})\right]^2+4\xi^2\left(\frac{\Omega}{2\omega_1}\right)^2} \tag{26b}$$

5.1.2 Nature of the coupled response

The exciting frequencies and exciting amplitudes, for which external resonance occurs, are known from section 3, so that the nature of the coupled response can be deduced by adding the curve corresponding to the threshold of coupled parametric resonance (26a) and (26b) into the diagram of external resonance (figure 2). Such a diagram is shown in figure 4 for the cable of the Ben Ahin Bridge studied previously (section 3.3), with an inclination of 30° and a damping ratio of 0.5 %. For this angle, Irvine's parameter becomes $\lambda^2 = 0.0544$ and the frequency of the first in-plane mode becomes $\omega_1^{in} = 7.84$ rad/s. The curve δ_{CU} represents the amplitude of the coupled threshold when coming from an uncoupled situation (26a), while the curve δ_{CC} represents the amplitude of the coupled threshold when coming from a coupled situation (26b). The curve δ_1 is the amplitude below which no external resonance occurs (14a) and below which the amplitude of the response is that of the lower branch of external resonance. The curve δ_2 indicates the amplitude above which external resonance occurs with certainty (14b) and above which the amplitude of the response is that of the upper branch of external resonance.

In figure 4, seven different regions can be distinguished:

- $\Omega < \Omega_{cr}$ and $\delta < \delta_{CU}$: The response is undifferentiated, the higher the frequency and the amplitude of excitation, the higher the amplitude of the response (region 1).
- $\Omega > \Omega_{cr}$ and $\delta < \delta_1$: No external resonance occurs, the response has a small amplitude (region 2).
- $\Omega > \Omega_{cr}$ and $\delta_2 < \delta < \delta_{CU}$: Only external resonance occurs with large amplitude

(region 3).

- $\Omega > \Omega_{cr}$ and $\delta_2 < \delta < \min(\delta_{CC}, \delta_2)$: Uncoupled hysteresis region. External resonance might occur alone, depending on the time history of the excitation; two amplitudes, one small and one large are possible for the response (region 4).
- $\Omega > \Omega_{cr}$ and $\delta_{CU} < \delta < \delta_2$: Coupled hysteresis region I. Coupled resonance might occur depending on the time history of the excitation. Two sets of amplitudes are possible: one uncoupled external resonance with low amplitude, coupled external and parametric resonances, both with high amplitudes (region 5).
- $\Omega > \Omega_{cr}$ and $\delta_{CC} < \delta < \delta_{CU}$: Coupled hysteresis region II. Coupled resonance might occur depending on the time history of the excitation (oscillation must come from an initial coupled situation). Two sets of amplitudes are possible and identical to those of the coupled hysteresis region I (region 6).
- $\Omega > \Omega_{cr}$ and $\max(\delta_{CU}, \delta_2) < \delta$: Coupled external/parametric resonance occurs with high amplitudes of the response of the first and second modes (region 7).

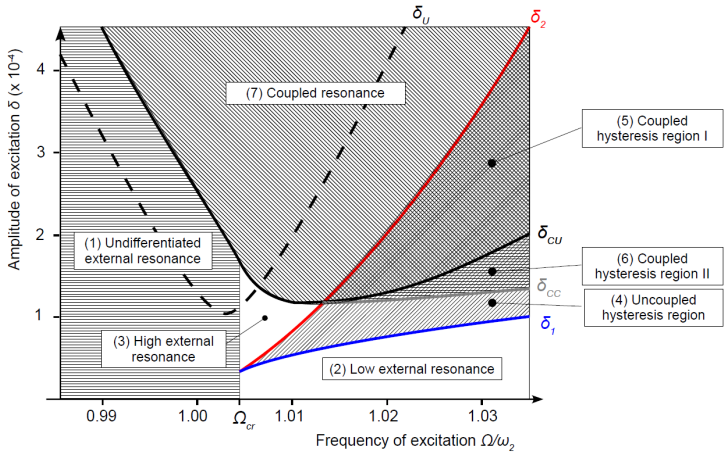

Figure 4: Nature of the response to coupled external/parametric resonance ($\xi = 0.5$ %).

Comparing then the amplitude of the uncoupled threshold δ_U (20) (dotted curve on figure 4) with the characteristic curves of the coupled thresholds δ_{CU} (26a) and δ_{CC} (26b) and those of the uncoupled hysteresis region δ_1 (14a) and δ_2 (14b), it is observed that the coupling causes a shift toward the high frequencies of the instability region, as well as a widening of this instability region. This widening is reduced by the hysteresis region but still, the coupled instability region remains wider than the uncoupled one. Taking the coupling into account seems, thus, necessary.

5.1.3 In-plane/out-of-plane interaction and numerical validation

To investigate the different thresholds, three different schemes are used for the time history of the excitation because of the hysteresis region:

- the "increasing low" scheme used to get the lower branch of external resonance: the amplitude grows slowly until it reaches the desired value, and then it remains constant until steady state.
- the "increasing high" scheme used to get the higher branch of external resonance before coupling appears: calculations start from a first run in which the frequency is out-of the hysteresis region and for which the exciting amplitude is below that of the threshold of coupled parametric resonance, the exciting frequency is increased until the desired one and then the amplitude until parametric resonance appears.
- the "decreasing coupled" scheme used to get the upper branch of external resonance with coupled external/parametric resonance: the amplitude starts from a high value

which is out-of the hysteresis range of coupled external/parametric resonance and remains constant until steady state takes place, then it is decreased slowly until it reaches the desired amplitude of excitation and remains constant until steady state.

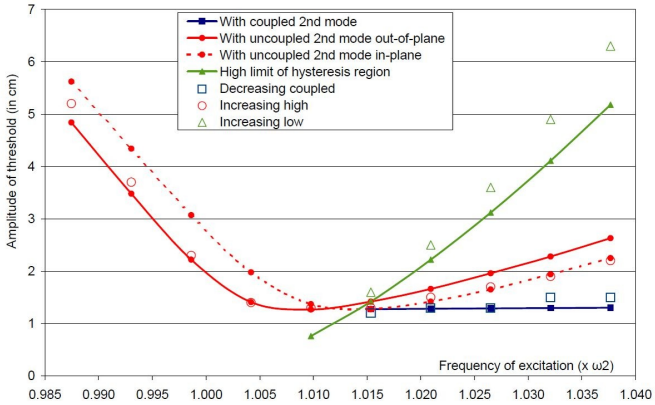

Figure 5: Thresholds of coupled external-parametric resonance out-of-plane.

Using these three time histories numerical values for the threshold have been determined and compared to analytical values obtained by expressions (26a), (26b) and (20). For the plane model, very good agreement of the various thresholds was found. The results for out-of-plane model are presented in figure 5 for the out-of-plane model. One observed that there is good agreement of the two thresholds and a slight underestimation of the amplitude of the high limit of the hysteresis region. It is however remarkable that, like for the horizontal cable, when the analytical value of the threshold of coupled in-plane parametric resonance is below that of coupled out-of-plane resonance, the numerical value of the out-of-plane threshold follows that of the in-plane threshold. In other terms, like for the horizontal cable, the first in-plane mode is unstable and almost vanishes when an out-of-plane perturbation is introduced. This time however, when the out-of-plane perturbation is introduced, the first out-of-plane mode settles slowly and finally dominates the response, but the first in-plane mode does not vanish completely. The second out-of-plane mode also accompanies the first out-of-plane mode, and indeed, develops more quickly (the interaction of these four modes is further discussed in section 5.3.2).

5.2 Coupled amplitudes and phases

5.2.1 Influence of the exciting amplitude

It is supposed now that the dimensionless amplitude of parametric excitation is above that of the threshold (26a) or (26b), which means that parametric resonance appears and that there is actually coupling between the first and second mode of vibration. The purpose of this subsection is to determine the amplitudes of coupled external and parametric resonance by solving simultaneously (8a) and (8b). The expression of parametric resonance (30) resulting from (8a) is introduced into (8b):

$$\begin{bmatrix} \frac{20}{3}c_3B^2+\omega_2^2-\Omega^2+2c_3A_U^2 & -\xi\omega_2\Omega \\ \xi\omega_2\Omega & \frac{20}{3}c_3B^2+\omega_2^2-\Omega^2+2c_3A_U^2 \end{bmatrix} \cdot \begin{bmatrix} p_{21} \\ p_{22} \end{bmatrix} = \begin{bmatrix} 0 \\ -\frac{\delta\cos\theta\Omega^2}{\pi} \end{bmatrix} \quad (27)$$

The above matrix can always be inverted. The coupled equations (27) are thus solved and combined, writing that $B^2=p_{21}^2+p_{22}^2$, in order to find the value of the amplitude of the vibration of the second mode:

$$\frac{400}{9}c_3^2B^6+\frac{40}{3}c_3\left(\omega_2^2-\Omega^2+2c_3A_U^2\right)B^4+\left[\left(\omega_2^2-\Omega^2+2c_3A_U^2\right)^2+\xi^2\omega_2^2\Omega^2\right]B^2=\frac{\delta^2\cos^2\theta\,\Omega^4}{\pi^2} \quad (28)$$

This equation differs a lot from that of the uncoupled problem (equation (11)). Again, it can be solved analytically by using Cardan's method, but developing it here is not meaningful, and it is used only for numerical analysis. Figure 6a, for example, shows the variations of the amplitude of the response with the amplitude of the excitation for an exciting frequency of $\Omega = \omega_2$. The damping ratio is 0.5 %. One notes that the exciting frequency is smaller than the critical frequency of external resonance, reducing the hysteresis region ($\Omega = \omega_2 < \Omega_{cr}$). Thus, it is verified that, below the threshold amplitude of coupled parametric resonance δ_{CU} (26a), the response is uncoupled and only the second mode is excited. Above this threshold, parametric resonance appears and the response is coupled. The amplitude of the second mode is lower than in the uncoupled situation (dotted line), which is reasonable because the second mode competes with the first mode.

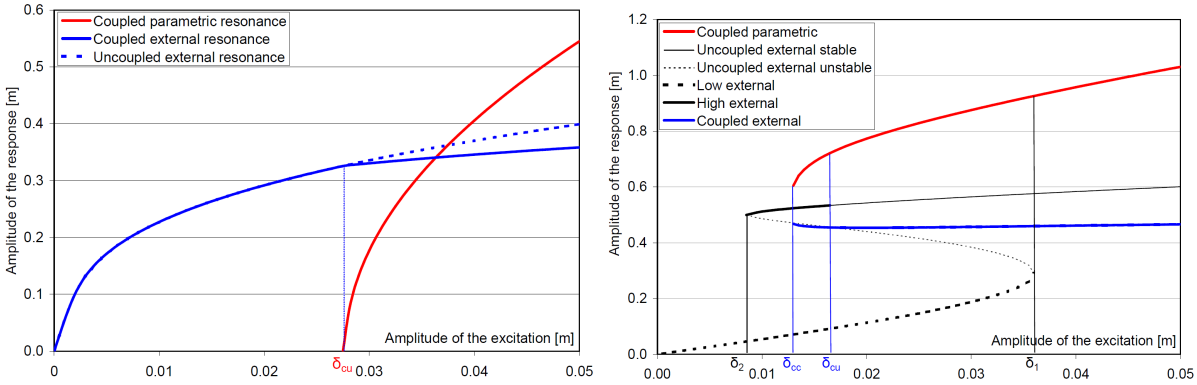

Figure 6: Influence of the exciting amplitude on the amplitude of coupled response, a) $\Omega = \omega_2$, b) $\Omega = 1.026\ \omega_2$.

When the frequency is higher than the critical frequency of external resonance, hysteresis phenomena appear and, for a given amplitude of excitation, many states of vibration can exist, depending on the time history of the vibration, as illustrated in figure 6b for $\Omega = 1.026\ \omega_2 > \Omega_{cr}$. It is noted that:

- $0 < \delta < \delta_2$: only low amplitude external resonance occurs (heavy dotted black curve).
- $\delta_2 < \delta < \delta_{CC}$: only external resonance occurs but it might have high (heavy full black curve) or low (heavy dotted black curve) amplitude.
- $\delta_{CC} < \delta < \delta_{CU}$: the response might be coupled external-parametric resonance (blue and red curves) if it is coming from a coupled situation or, otherwise, uncoupled with external resonance only, either high or low amplitude (heavy full and dotted black curve respectively).
- $\delta_{CU} < \delta < \delta_1$: the response might be coupled (blue and red curves) if coming from a coupled situation or from a situation with high amplitude of the second mode or, otherwise, it might be uncoupled with low amplitude external resonance only (heavy dotted black curve).
- $\delta_1 < \delta$: only coupled external-parametric response occurs.

5.3. Numerical validation with ADINA

5.3.1 Influence of the amplitude of excitation

To validate the analytical results presented above, purely plane simulations are conducted, as well as three dimensional simulations by introducing a small out-of-plane perturbation into the plane model. Figures 7a and 7b show the amplitude of external resonance and the

amplitude of parametric resonance, respectively. The exciting frequency is here $\Omega = 1.004\ \omega_2$. Before parametric resonance occurs, the system is uncoupled and there is excellent agreement between the numerical simulations and the analytical model (figure 7a). In figure 7b, it is observed that the threshold amplitudes of parametric resonances almost coincide for the in-plane model as well as for the out-of-plane model. The numerical threshold out-of-plane is between 14 mm and 15 mm while the analytical model gives $\Delta^{thr} = 14.0$ mm, and the threshold in-plane is between 20 mm and 21 mm while analytically $\Delta^{thr} = 19.7$ mm.

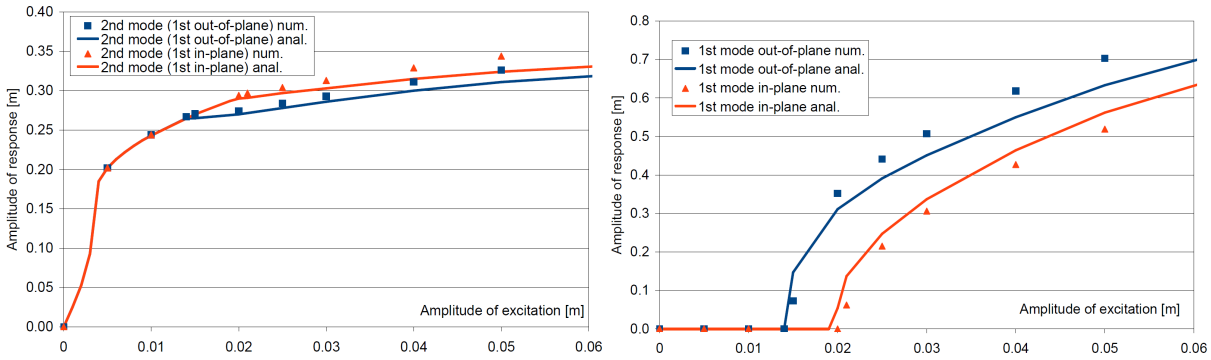

Figure 7: Comparison of analytical and numerical amplitudes of a) external resonance, b) parametric resonance.

Looking now at the amplitudes of response, once parametric resonance has appeared, the numerical in-plane parametric resonance response values are slightly below the analytical ones, contrary to the numerical out-of-plane amplitudes, which are slightly higher than the analytical ones. This is in accordance with the facts that the numerical threshold in-plane is higher than the analytical threshold, and that the numerical threshold out-of-plane is smaller than the analytical one. Moreover, in figure 7a, it is observed that the analytical model slightly underestimates the amplitude of coupled external resonance (about 2 % for $\Delta = 20$ mm and 5 % for $\Delta = 100$ mm). In these two figures the agreement of the analytical and numerical results can be described as very good for small exciting amplitudes and as satisfactory for higher amplitudes.

5.3.2 Influence of the frequency of the excitation

Another set of numerical experiments is conducted to study the influence of the exciting frequency for a fixed exciting amplitude, here $\Delta = 20$ mm. The exciting frequency was increased from 0.98 ω_2 to 1.04 ω_2 and decreased from 1.04 ω_2 to 1.01 ω_2 with a step of 0.005 ω_2, each frequency being kept constant during 1000 cycles for the steady state to install. The results are presented in figure 8a. The curves (analytical model) and dots (numerical simulations) fit remarkably well for growing and decreasing exciting frequency.

A similar set of experiments with $\Delta = 20$ mm and $\xi = 0.5$ % is then conducted numerically for the out-of-plane response for both increasing and decreasing frequencies from 0.98 ω_2 to 1.04 ω_2 introducing again a small out-of-plane perturbation at time zero (see figure 8b and figure 9). One remarks first that, like for the horizontal cable (section 4.2.2), the out-of-plane perturbation causes an instability of the in-plane mode, so that the first in-plane mode vanishes and the first out-of-plane mode dominates the steady state response. However, for high frequencies, the coupled out-of-plane response becomes more complex and may have nonzero components for up to four eigenmodes (see figure 9). Depending on the frequency and on the history of excitation different states might exist:

- The first one corresponds to low frequencies below that of resonance ($\Omega < \omega_2$), where response of the cable is purely external in-plane resonance.
- The second one is a bi-modal vibration state where out-of-plane parametric resonance is coupled with in-plane external resonance. It occurs for a relatively reduced

bandwidth ($\omega_2 < \Omega < 1.01\ \omega_2$).

– The third one involves the first four eigenmodes and occurs also for a reduced bandwidth ($1.01\ \omega_2 < \Omega < 1.02\ \omega_2$).
– The fourth one corresponds to the hysteresis region ($\Omega > 1.02\ \omega_2$) where the response might be either that of purely uncoupled in-plane resonance (dotted lines in figure 9), or a four modes coupled response, in which the coupling between the four modes is very strong.

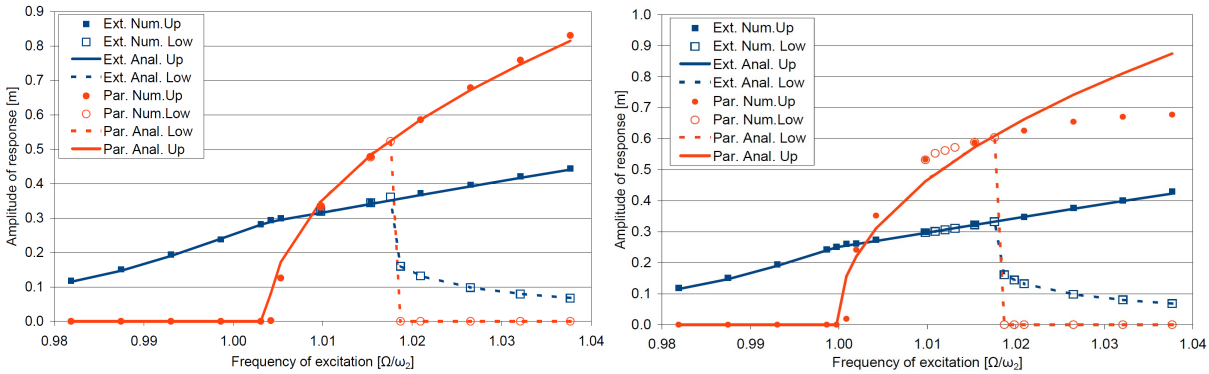

Figure 8: Influence of the excitation frequency on a) the in-plane coupled response, b) the out-of-plane response.

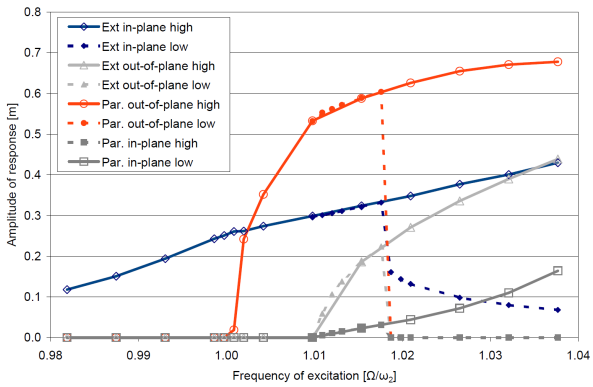

Figure 9: Influence of the excitation frequency on the number of modes in the out-of-plane coupled response.

It is hence clear that the two modes interaction analytical model presented here can not capture the whole response of the inclined cable because it involves up to four modes. However, it is noted in figure 8b that there is very good agreement between the amplitudes of the analytical model and the numerical simulations for the second in-plane mode. One thus deduces that in-plane external resonance is not affected by the presence of the first in-plane and second out-of plane modes, so that, practically, the two modes interaction is valid for external resonance. One observes then that the threshold of coupled out-of-plane parametric resonance is correctly predicted by the analytical model as well as the threshold of the hysteresis region. Moreover, in the regions where the response has only two non-zero components or a small contribution of the second out-of-plane mode ($\omega_2 < \Omega < 1.02\ \omega_2$), the analytical model fits relatively well with numerical results.

It is therefore considered that the two modes interaction model captures the main characteristics of the response and is sufficient for practical structural design purposes. Considering the fact that for $1.01\ \omega_2 < \Omega < 1.02\ \omega_2$, the amplitude of the first in-plane mode is small when compared to that of the other eigenmodes, the three modes interaction model of Gonzalvez-Buena *et al.* [21] is satisfactory and it can be used to determine the value of the threshold of the second out-of-plane mode. For higher frequencies, it is necessary to refer to

the general four modes interaction of Rega [23].

6. CONCLUSION

The objective of the present work was to propose the simplest possible analytical model for the proper investigation of coupled external/parametric resonance in order to bridge the gap between complex mathematical interaction models and practical design of cables in structural engineering. To this end, abundant numerical applications and simulations were conducted for realistic values, based on actual bridge cables. Two specific cases were first investigated to gain better understanding of the two resonance phenomena separately. The first one was dedicated to external resonance and dealt with a horizontal cable submitted to a vertical harmonic motion at one end. Most of the existing results on the phenomenon were re-established analytically (in particular the limits of the hysteresis region) and confirmed numerically. The second specific case was dedicated to parametric resonance and dealt with a horizontal cable submitted to a horizontal harmonic motion at one end. Again, most of the existing results on parametric resonance were re-established analytically and confirmed numerically. Moreover it was observed that, when disturbed out-of-plane, the in-plane parametric resonance was unstable and turned into out-of-plane parametric resonance, so that only out-of-plane parametric resonance is stable and its bandwidth is formed by the disjunction of the in-plane and out-of-plane bandwidth.

Then, the coupling phenomenon strictly speaking was investigated, focusing on a cable with a 30° inclination. Analytical expressions for the coupled amplitudes were developed and their comparison with numerical simulations showed very good agreement. The study has proved that the coupling shifts the bandwidth of parametric resonance toward the higher frequencies and diminishes the value of the threshold when the frequency is above that of resonance. However, very strong interaction between the hysteresis regions of the two resonances has been found. Indeed, parametric resonance requires a high amplitude of external resonance to take place, so that one could say that it is necessary that external resonance appears first to cause parametric resonance. Concerning amplitudes, when coupling appears, it diminishes both, the amplitude of external and parametric resonance.

Moreover, numerical simulations showed that the introduction of an out-of-plane perturbation led to coupled out-of-plane vibrations so that, like for the horizontal cable, the only stable parametric resonance is the out-of plane of which the instability bandwidth might be considered in a first approximation as formed by the disjunction of the in-plane and out-of-plane bandwidth. However, it has been shown that, under certain conditions, the coupling phenomenon might involve up to four eigenmodes: the first in-plane and out-plane and second in-plane and out-of-plane modes. It has been also shown that the additional vibration modes only partially affect the amplitude of the main eigenmodes in the frequency domain useful for the engineer, for frequencies out-of the hysteresis range.

REFERENCES

[1] Kumarasena S., Jones N.P., Irwin P., Taylor P., Wind-Induced Vibration of Stay Cables, Office of Infrastructure R&D, Fed. Highway Adm., FHWA-RD-05-083, 284 pages, 2007.
[2] SETRA, Haubans, Recommandations de la commission interministérielle de la précontrainte, 200 pages, 2001.
[3] Irvine M., Cable structures, The MIT press, 1981.
[4] Caetano E., Indirect excitation of stays on cable-stayed bridges, in Proceedings of the 4th international symposium on cable dynamics, Montréal, Canada, 2001, 129-136.
[5] Caetano E., Cable vibrations in cable-stayed bridges, IABSE, 188 pages, 2007.
[6] Kovacs I., Zur Frage der Seilschwingungen und der Seildämpfung, Die Bautechnik 1982; 325-332.

[7] Uhrig R., On kinetic response of cable of cable-stayed bridges due to combined parametric and forced excitation, Journal of sound and vibration (JSV) 1993; 165(1): 185-192.
[8] Lilien J., Pinto da Costa A., Vibrations amplitude caused by parametric excitation of cables stayed structures, JSV 1994, 174(1): 69-90.
[9] Cai Y., Chen S., Dynamic of elastic cable under parametric external resonances, Journal of engineering mechanics 1994; 120(8): 1786-1802.
[10] Clément H., Crémona, C.: Étude mathématique du phénomène d'excitation paramétrique appliquée aux haubans de pont, in Études et recherches des laboratoires des ponts et chaussées, OA18, LCPC, Paris, 1996.
[11] Berlioz A. and Lamarque C.H., A non-linear model for the dynamics of an inclined cable, JSV 2005; 279: 619-639.
[12] Takahashi K., Dynamic stability of cables subjected to axial periodic load, JSV 1991, vol. 144, n 2, 323-330.
[13] Rega G.,Nonlinear vibrations of suspended cables - Part I: Modeling and analysis, Applied Mechanics Reviews (ASME) 2004; 57(6): 443-478.
[14] Nayfey A., Mook D., Non linear oscillations, ed. John Wiley and sons, USA, 1979.
[15] Luongo A, Rega G., Vestroni F., Monofrequent oscillations of a non-linear model of a suspended cable, JSV 1982; 82: 247-259.
[16] Al-Noury S.I., Ali S.A., Large amplitude vibrations of parabolic cables, JSV 1985; 101: 451-462.
[17] Takahashi K., Konishi Y., Nonlinear vibrations of cables in three dimensions. Part II: out-of-plane vibration under in-plane sinusoidally time varying loading, JSV 1987; 118: 85-97.
[18] Visweswara Rao G., Iyengar R. N., Internal resonance and non-linear response of a cable under periodic excitation, JSV 1991; 149(1): 25-41.
[19] Benedettini F., Rega G., Non-linear dynamics of an elastic cable under planar excitation. International Journal of non-linear mechanics 1987; 22: 497.
[20] Perkins N.C., Modal interactions in the non-linear response of elastic cables under parametric/external excitation, Journal of non-linear mechanics 1992; 27(2): 233-250.
[21] Gonzalez-Buelga A., Neidl S.A., Wagg D.J., Macdonald S.H.G, Modal stability of inclined cables subjected to vertical support excitation, JSV 2008; 318: 565-579.
[22] Chatjigeorgiou I.K., Mavrakos S.A., Nonlinear resonances of parametrically excited risers, numerical and analytic investigation for $\Omega = 2\omega_1$, Comp. & Str. 2005; 83: 560–573.
[23] Benedettini F., Rega G., Alaggio R., Non-linear oscillations of a four degrees of freedom model of a suspended cable under multiple internal resonance conditions, JSV 1995; 182(5): 775-798.
[24] Zhang W., Tang Y., Global dynamics of the cable under combined parametric and external excitations, International Journal of Non linear mechanics 2002; 37: 505-526.
[25] Srinil N., Rega G., Space-time numerical simulation and validation of analytical predictions for nonlinear forced dynamics of suspended cables, JSV 2008; 315: 394–413.
[26] Srinil N., Rega G., Two-to-one resonant multi-modal dynamics of horizontal/inclined cables: Part II: Internal resonance activation, reduced-order models and non-linear normal modes. Nonlinear Dynamics 2008; 48: 253-274.
[27] McClure G., Lapointe M., Modeling the structural dynamic response of overhead transmission lines, Computers and Structures 2003; 81: 825–834.
[28] Vassilopoulou I., Gantes C. J., Vibration modes and natural frequencies of saddle form cable nets, Computers and Structures 2010; 88 (1-2): 105-119.